Coastal Winds in South Florida

GE PENG

Division of Meteorology and Physical Oceanography, Rosenstiel School of Marine and Atmospheric Science, University of Miami, Miami, Florida

CHRISTOPHER N. K. MOOERS

Ocean Prediction Experimental Laboratory and Division of Applied Marine Physics, Rosenstiel School of Marine and Atmospheric Sciences, University of Miami, Miami, Florida

HANS C. GRABER

Division of Applied Marine Physics, Rosenstiel School of Marine and Atmospheric Science, University of Miami, Miami, Florida

(Manuscript received 14 April 1998, in final form 16 February 1999)

ABSTRACT

Thirteen-month records for the period of April 1994–April 1995 from eight (out of nine) Coastal-Marine Automatic Network (C-MAN) stations in south Florida are analyzed statistically to study alongshore variability of observed atmospheric variables. The surface variables largely are statistically homogeneous and coherent along the Straits of Florida. The maximum correlation for hourly wind components between adjacent stations (separated alongshore by 30–117 km) ranges from 0.9 to 0.75, respectively. However, there is a lack of coverage in the cross-shore direction; hence, a redistribution of C-MAN stations in the cross-shore direction should be considered to provide better spatial coverage of surface atmospheric variables in the south Florida region.

Surface winds from the National Centers for Environmental Prediction (NCEP) 80-km grid, η (Eta) Model analysis for the same period are compared statistically with observations from an air–sea interaction buoy and a C-MAN station in the south Florida coastal region. The η winds represent the low-frequency winds (periods between 3 days and 3 weeks) fairly well (e.g., the coherence exceeds 0.8 and the phase difference is less than 15°) but generally are weaker in magnitude than are the observed winds. The difference can be up to 2 m s^{-1} for the monthly mean and 1 m s^{-1} for the seasonal mean. The histogram of the η winds in winter has a single large peak instead of multiple peaks as occur in those of the observed winds. Southward bias in the η winds exists in summer.

The η Model simulates well the flow patterns of a tropical cyclone and an extratropical cyclone on the regional scale but lacks local spatial variability. As demonstrated, local spatial variability can be represented better by a blend of model and observed winds than by either the model-based or observed local surface winds alone.

These issues need to be reexamined periodically with upgraded versions of NCEP's operational models.

1. Introduction

Accurate surface winds over south Florida are crucial to making accurate local weather forecasts that involve multiscale motion (i.e., trade winds, synoptic-scale winds, sea–land and lake breezes, as well as cloud-scale winds and high-frequency winds associated with local convective cells and vegetation variations) (Cooper et al. 1982; Segal et al. 1988).

Accurate surface winds (in terms of wind intensity and structure) also are essential for driving oceanic circulation models to produce accurate wind-driven surface currents that are crucial to marine transport, larvae fish dispersion, pollutant transport, and humanistic missions such as search and rescue. South Florida's coastal oceanic circulation is also a complex and multiscale system. The Yucatan Current enters the Gulf of Mexico from the Caribbean Sea and curves clockwise as the Loop Current before exiting the Gulf through the Straits of Florida as the Florida Current, which flows along the east coast of Florida and becomes the Gulf Stream. The Loop Current sheds large-scale eddies and is also a source for meso- and small-scale eddies that impact the south Florida coastal ocean. Those eddies result from

Corresponding author address: Dr. Ge Peng, MPO/RSMAS, University of Miami, 4600 Rickenbacker Causeway, Miami, FL 33149-1098.
E-mail: gpeng@rsmas.miami.edu

instability and interaction among multiscale systems (Fratantoni 1998). Thus, predicting realistic coastal flow is, without doubt, an important but difficult task. Numerical simulations have shown that the coastal ocean response can be very sensitive to the resolved wind structure in the Gulf of Mexico (Mooers et al. 1998, manuscript submitted to *J. Geophys. Res.*) and Straits of Florida (Mooers and Ko 1994). The uncertainties in the surface wind fields are the largest source of errors in ocean model–generated analyses (Cardone et al. 1990). More generally, the responsiveness of the coastal ocean to atmospheric forcing as a function of spatial scales and timescales is not well known; however, it is an active area of research that is becoming feasible with improved in situ and space-based observing systems, plus high-resolution mesoscale atmospheric models and numerical weather prediction systems. Here, a few innovative steps in analyzing the wind forcing that operates on south Florida are taken in preparation for simulations of the coastal ocean's response.

Surface winds are provided operationally by National Weather Service (NWS) stations[1] distributed over the south Florida region. They have been used to study regional-scale motions such as sea–land and lake breezes (Byers 1948; Burpee 1979; Lyons et al. 1992) and convective development as a result of synoptic-scale wind variations and the lake effect (Cunning et al. 1982). Typical south Florida wind and thunderstorm patterns also have been examined extensively (Blanchard and López 1985; Michaels et al. 1987; Pielke et al. 1990). The NWS winds, generally sampled every 12 h, are not able to resolve most mesoscale motions, and lack spatial resolution. In addition, virtually no wind measurements were provided along the coast until the 1980s, when the Coastal-Marine Automated Network (C-MAN) was established along the coast of the United States. Although some basic statistical analyses are done routinely with C-MAN observed variables at the National Data Buoy Center (NDBC) during the data quality-control phase, statistical characteristics of the network and alongshore variability of its observations for south Florida have not been documented in the literature. Such a study is necessary for researchers to use observed variables from the network in air–sea interaction and ocean model studies as well as for managers to make sensible decisions on how to maximize the information that the south Florida C-MAN can provide.

As regional numerical models and mesoscale process parameterizations (including cloud physics) improve and as computer power increases rapidly, regional model-analyzed and -forecasted winds are routinely available to the weather forecast and research communities. How good are these model-based winds when compared to observations on the local scale? Are they biased in any way? To be confident in using these model-based winds, the above questions need to be addressed. If the model-based winds are routinely good, does there remain a need for the local surface observation network, especially in view of the cost to maintain it?

In this study, coastal winds observed at C-MAN stations along the east coast of south Florida are first analyzed statistically in section 2. Then, winds from the National Centers for Environmental Prediction (NCEP) η (Eta) Model are compared statistically with local observed winds in section 3. Two case studies (Tropical Storm Gordon and an extratropical cyclone) are used in section 4 to investigate how well the regional η model describes typical synoptic events and to explore the benefits of blending local observations with the model fields. Last, the results are summarized in section 5.

2. Statistical characteristics of south Florida C-MAN data

The C-MAN was established in the 1980s to provide surface atmospheric information (e.g., wind, pressure, air temperature), sea surface temperature, and other oceanic information (e.g., conductivity for salinity; wave height and period) at selected stations to meet the needs of forecasters who issue watches and warnings and to support studies of the Florida coastal ecology (NDBC 1993; Bosart and Sprigg 1998). Eight stations are aligned along the east coast of south Florida (from Dry Tortugas to Settlement Point, Bahamas) (top of Fig. 1). There is only one station located on the west coast of south Florida (Venice, which is not included in this study because of a 3-month data gap). The distance between station pairs ranges from 30 to 485 km (bottom of Fig. 1). The network has provided valuable data to both the forecasting and the research communities (Maul et al. 1991; Ortner et al. 1995; Ogden et al. 1994; Wang et al. 1994) since it plays an important role in the availability of operational atmospheric and oceanic observations in the south Florida coastal region. The first systematic study of this network is presented here. This section describes some of the statistical aspects of the C-MAN observations to set the stage for the next section where year-long records of surface winds (from the NCEP η model, an air–sea interaction buoy, and the C-MAN network) are examined to determine whether the observed statistical characteristics are well represented in the NCEP regional operational analysis and forecast system.

a. Data

The hourly C-MAN data are obtained from NDBC. The competely automated quality-control procedures are performed at the NWS Telecommunication Gateway (NWSTG) before data are submitted for archival at NDBC, where an additional human–machine quality-

[1] Currently, the NWS stations over the south Florida region are located at Tampa, Melbourne (no upper-air report), Fort Myers (no upper-air report), Key West, Naples (no upper-air report), and Miami.

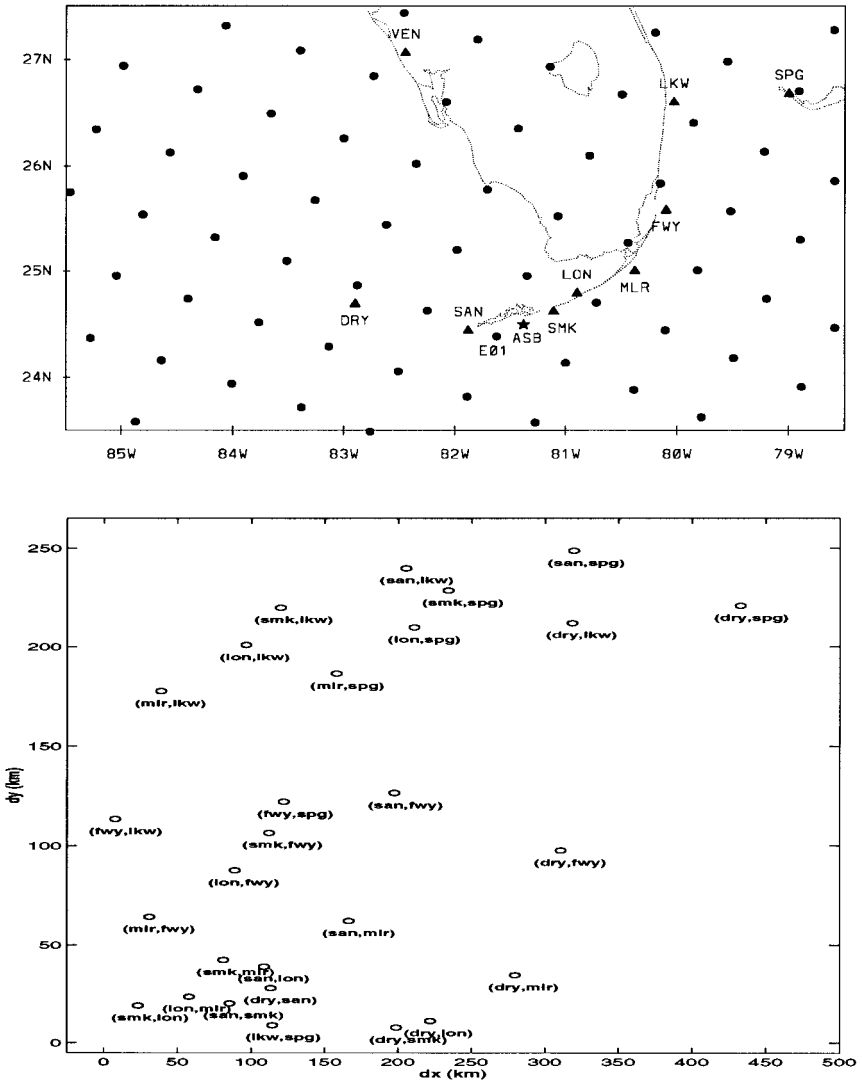

FIG. 1. Map of data sites in the south Florida region (upper panel). Dot: η Model grid points; triangle: C-MAN stations; asterisk: air–sea interaction buoy. The NWS stations are not plotted here. Separation distance (km) between C-MAN station pairs (lower panel). Here, *dx* and *dy* are distances in the east–west and north–south directions, respectively. Station definitions are given in Table 2.

control procedure is performed (Gilhousen 1988). The quality-control procedures detect and eliminate instrumental errors, gross errors, and transmission parity errors. A procedure that checks ranges of observed variables and time continuity limits is performed at both NWSTG and NDBC. A similar procedure is performed locally to ensure further the quality of the data.

The dataset extends from 1 April 1994 to 30 April 1995 (Table 1; complete and abbreviated names of the stations are given in Table 2). Gaps in the data continuity range from one hour to a month along the east coast of south Florida. Data gaps are filled by a weighted interpolation of the values from adjacent stations. The weighting function is based on Cressman (1959) with an *e*-folding length scale of 300 km, which yields the best fit.

The large missing data percentages at Fowey Rocks and Venice result from data gaps of a month or longer (22 June–22 July 1994 for Fowey Rocks and 5 October 1994–9 January 1995 for Venice). The Venice station data are excluded from this study because of the large amount of missing data, though the cross-coast variability may be as important as alongcoast variability.

b. Adjustment of C-MAN wind data

Most C-MAN wind sensors are not mounted at the standard marine boundary layer height of 10 m for sur-

TABLE 1. Summary of the data and station attributes: 1 Apr 1994–30 Apr 1995. Eta (η) is an Eta Model grid point. ASB is an air–sea interaction buoy. Installation year: 93 = 1993, etc.

Attribute	Station identifier (see Table 2)									
	e01	asb	smk	san	dry	lon	mlr	spg	fwy	lkw
Data type	η	ASB	C-MAN							
Timescale	12 hourly	hourly	hourly							
Location	24.40	24.51	24.63	24.45	24.70	24.80	25.01	26.69	25.59	26.61
(°N/°W)	81.62	81.38	81.11	81.88	82.90	80.90	80.38	79.00	80.10	80.03
Installed (month/year)	6/93	3/94	9/88	10/92	10/92	10/92	2/88	10/85	12/87	7/84
Sensor height (m)	10	3	48.5	13.6	6.4	6.1	15.9	9.8	43.9	7.6
No. missing	82	63	69	140	80	167	83	659	946	374
No. records	708	9417	9411	9340	9400	9313	9397	8821	8534	9106
No. missing/total (%)	10.38	0.65	0.73	1.48	0.84	1.76	0.88	6.95	9.98	3.95

face wind measurement (Table 1). Therefore, a dynamical procedure is performed to adjust the observed C-MAN wind speed to the 10-m equivalent wind speed. This procedure uses a boundary layer profile scheme (Cardone 1969; Ross et al. 1985). The effective wind speed is defined as

$$U_e(z) = \frac{U_*}{k}\left[\log\left(\frac{z}{z_0}\right) - \phi_m\left(\frac{z}{L}\right)\right], \quad (1)$$

where z is the height above mean sea level. Here, U_* is friction velocity, which characterizes the wind profile in the marine surface layer and depends on the reported wind speed and air–sea temperature difference; k is the von Kármán constant, ranging from 0.38 to 0.42 (0.4 is used here); z_0 is a roughness parameter (i.e., roughness height), generally an empirical function of U_* in the surface boundary layer; ϕ_m is the nondimensional wind shear, which is a function of the dimensionless ratio z/L; and L (the Monin–Obukhov length) is a scaling factor defined as

$$L = \rho C_p U_*^3/kgH, \quad (2)$$

where H is the heat flux (positive from sea to air), ρ is the air density, g is gravitational acceleration, and C_p is the specific heat of air at constant pressure. For further description of the algorithm and the general procedure, see Cardone et al. (1995).

TABLE 2. Abbreviated and complete names of the south Florida C-MAN stations.

dry	Dry Tortugas
lon	Long Key
lkw	Lake Worth
san	Sand Key
mlr	Molasses Reef
spg	Settlement Point
smk	Sombrero
fwy	Fowey Rocks
ven	Venice

c. Statistical analyses

1) TIME SERIES, MEANS, VARIANCES, AND HISTOGRAMS

At this point, several statistical definitions used in this study are defined. After Taylor (1982) and Press et al. (1992),

$$\overline{x} = \frac{1}{N}\sum_{i=1}^{N} x_i = \text{mean};$$

$$\sigma_x = \sqrt{\frac{1}{N-1}\sum_{i=1}^{N}(x_i - \overline{x})^2}$$

$$= \text{sampled standard deviation (STD)};$$

$$\sigma_{\overline{x}} = \frac{\sigma_x}{\sqrt{N}} = \text{standard deviation of mean or SDOM};$$

$$\text{frac (\%)} = 100\frac{\sigma_{\overline{x}}}{|\overline{x}|} = \text{fractional uncertainty},$$

where $x_1, x_2, \ldots, x_N$ are N separate measurements of variable x.

The standard deviation estimates the spread of the measurements in reference to the mean. The uncertainties of random errors in the measurements are represented by the SDOM, which gives the absolute uncertainty. The fractional uncertainty gives the relative uncertainty.

Both air temperature and sea surface temperature time series show a distinct seasonal cycle (Figs. 2a,b), while air temperature undergoes larger fluctuations associated with synoptic events (e.g., cold front and tropical storm passages) than sea surface temperature does. The manifestations of cold front passages (i.e., sharp and strong pressure drops) are pronounced in surface pressure time series (Fig. 2c). The annual cycles for wind components are not distinct (Figs. 2d,e) since the winds largely are influenced by synoptic-scale and mesoscale motions that are highly variable. However, the easterly (westward) wind prevails all year (Table 3) with a weak southerly (northward) component in the summer months and

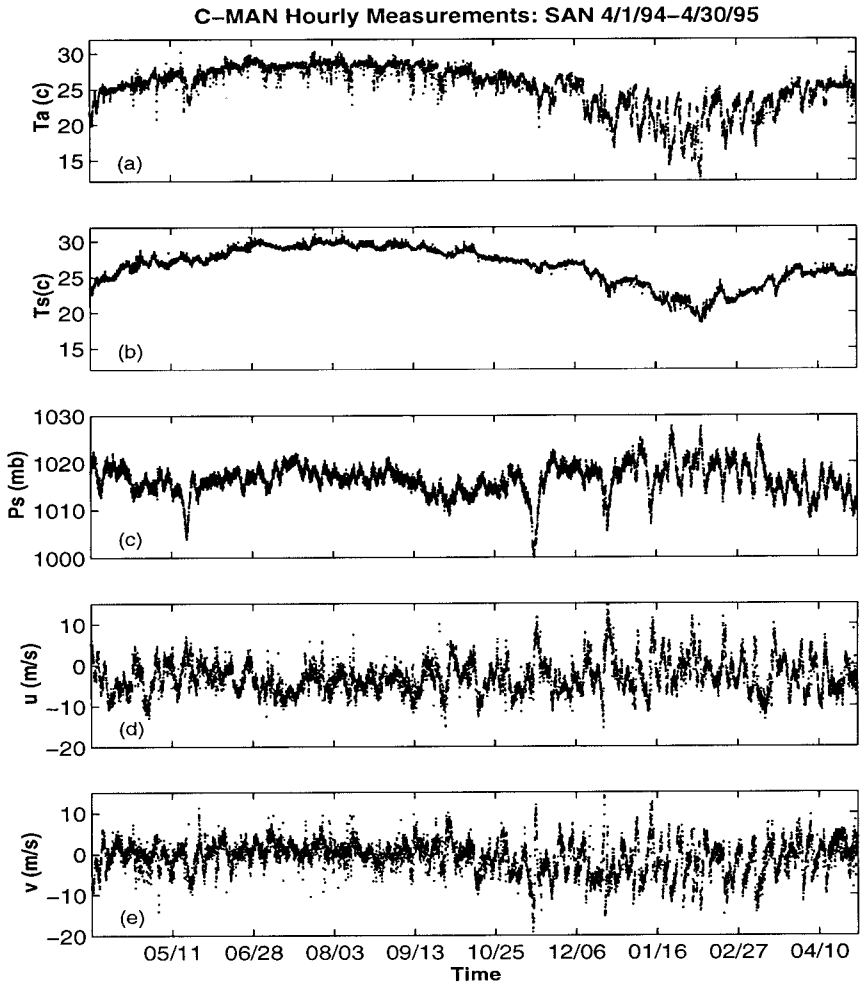

FIG. 2. Time series at Sand Key of (a) air temperature; (b) sea surface temperature; (c) surface pressure; (d) surface u component; and (e) surface v component. See Peng et al. (1996) for time series at other C-MAN stations.

northerly (southward) component in the winter months (Fig. 3). The monthly mean wind experiences sharp direction changes in the late spring and late autumn. The spatial variations of the monthly mean winds are much more pronounced in winter than in summer. The monthly variances are lowest in June and July with an average value of 5 $m^2\ s^{-2}$. The maximum monthly variances occur mostly in December and January with an average value of 30 $m^2\ s^{-2}$. There is another peak in March for the u (zonal) component (Peng et al. 1996).

The absolute uncertainties of the measurements for all the variables are low; so are the relative uncertainties except for the meridional velocity (fractional uncertainty of up to 21%; see Table 3). Those large relative uncertainty values may be alarming but not too surprising for the following reasons. Since the easterly winds prevail

TABLE 3. Station identifier, mean, standard deviation of the mean, and fractional uncertainty.

Station ID	$\overline{u}$ (m s^{-1})	$\sigma_{\overline{u}}$	Frac (%)	$\overline{v}$ (m s^{-1})	$\sigma_{\overline{v}}$	Frac (%)
dry	−2.17	0.036	1.66	−1.05	0.035	3.34
san	−2.97	0.041	1.38	−0.96	0.041	4.26
smk	−2.70	0.040	1.48	−0.39	0.040	10.31
lon	−2.68	0.040	1.48	−0.19	0.040	21.00
mlr	−2.48	0.042	1.70	0.35	0.042	11.78
fwy	−2.11	0.048	2.26	0.52	0.040	7.60
lkw	−1.97	0.041	2.10	0.34	0.041	12.13
spg	−1.71	0.037	2.18	0.26	0.030	11.64

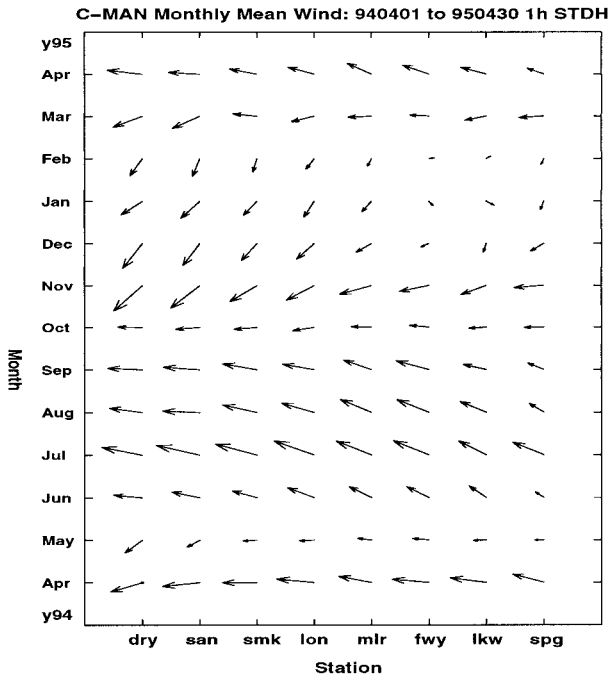

FIG. 3. Monthly mean wind vectors for all eight C-MAN stations from Apr 1994 to Apr 1995.

all year, the meridional velocity is mainly a perturbation from synoptic systems superimposed onto the (zonal) mean wind. In addition, instrumental precision is about 0.05 m s^{-1}, which is of the order of the absolute uncertainties; thus, measurement precision can be a major contributing factor to the large relative uncertainties.

The wind speed histograms are similar at most of the stations except Dry Tortugas and Settlement Point (Fig. 4a). The most frequent wind speed is slightly higher at Dry Tortugas and substantially lower at Settlement Point. The wind direction histograms also are similar (Fig. 4b). The easterly peak (near 90°) for Lake Worth is reduced by about 30%; the northwesterly peak (near 315°) is generally higher at this station than at any other station. Hence, Dry Tortugas (located at the far western end of the straits) and Settlement Point (located at the northern end of the straits) provide additional information that is unique compared to that provided by the other six stations, which are located between them along the Straits of Florida.

2) AUTOSPECTRA AND AUTOCORRELATION FUNCTIONS

As is to be expected, there is more energy at the low frequencies than at the high frequencies in the ensemble mean rotary spectra (Mooers 1973) of horizontal velocity (Fig. 5; see Peng et al. 1996 for individual total wind spectra not shown here). Distinct peaks are shown at the diurnal and semidiurnal frequencies in both clockwise and anticlockwise spectra. A broad peak in the synoptic scale (period of 4–7 days) appears in the anticlockwise spectrum.

The autocorrelation functions of winds are dominated by synoptic-scale motions; however, they also are influenced by the seasonal cycle, particularly for the v (meridional) component (Peng et al. 1996). The maximum cross correlation of adjacent station pairs occurs at zero lag and is quite high, ranging from 0.9 to 0.75 over separation distances of 30–117 km (Fig. 6). The maximum correlation between station pairs decreases as the station separation increases, reaching 0.6 at about 485 km for both components.

d. Discussion

The statistical properties of the surface variables at the eight C-MAN stations largely are spatially homogeneous, more so from Sand Key to Lake Worth (encompassing the innermost six stations). There is a great similarity in wind speed and direction histograms and monthly mean winds among the Sand Key, Sombrero, Long Key, and Molasses stations. Thus, one or two of these stations might profitably be moved to the western side of Florida Bay or the west coast of south Florida. Since the correlation between adjacent station pairs is quite high as noted above, a modest redistribution of C-MAN stations could provide better coverage of the cross-shore spatial structure of surface variables without loss of important alongshore information. In part, such additional information can be obtained through local conventional meteorological stations managed by the NWS as well as from regional operational atmospheric circulation models (for example, the NCEP η Model). Meteorological buoys deployed in the south Florida region also may contribute to the needed information. In the next section, the 80-km η Model wind analysis will be verified by comparison with observations from the south Florida surface observation network. The spectral and correlation properties of the η Model surface values will be assessed versus the south Florida surface observation network for the quality of their information content at seasonal and synoptic scales.

3. The η Model analysis versus observations

Since the orography basically is flat, its influence on south Florida weather is negligible, which makes south Florida an ideal place to examine how well a model treats multiscale atmospheric processes and whether a model provides adequate atmospheric forcing to eddy-resolving coastal oceanic circulation models, without having to deal with orographic effects explicitly. In addition, the south Florida surface observation network, which consists of eight C-MAN stations and an air–sea interaction buoy (ASB), provides in situ wind measurements during the period of focus here that can be used to verify the model output.

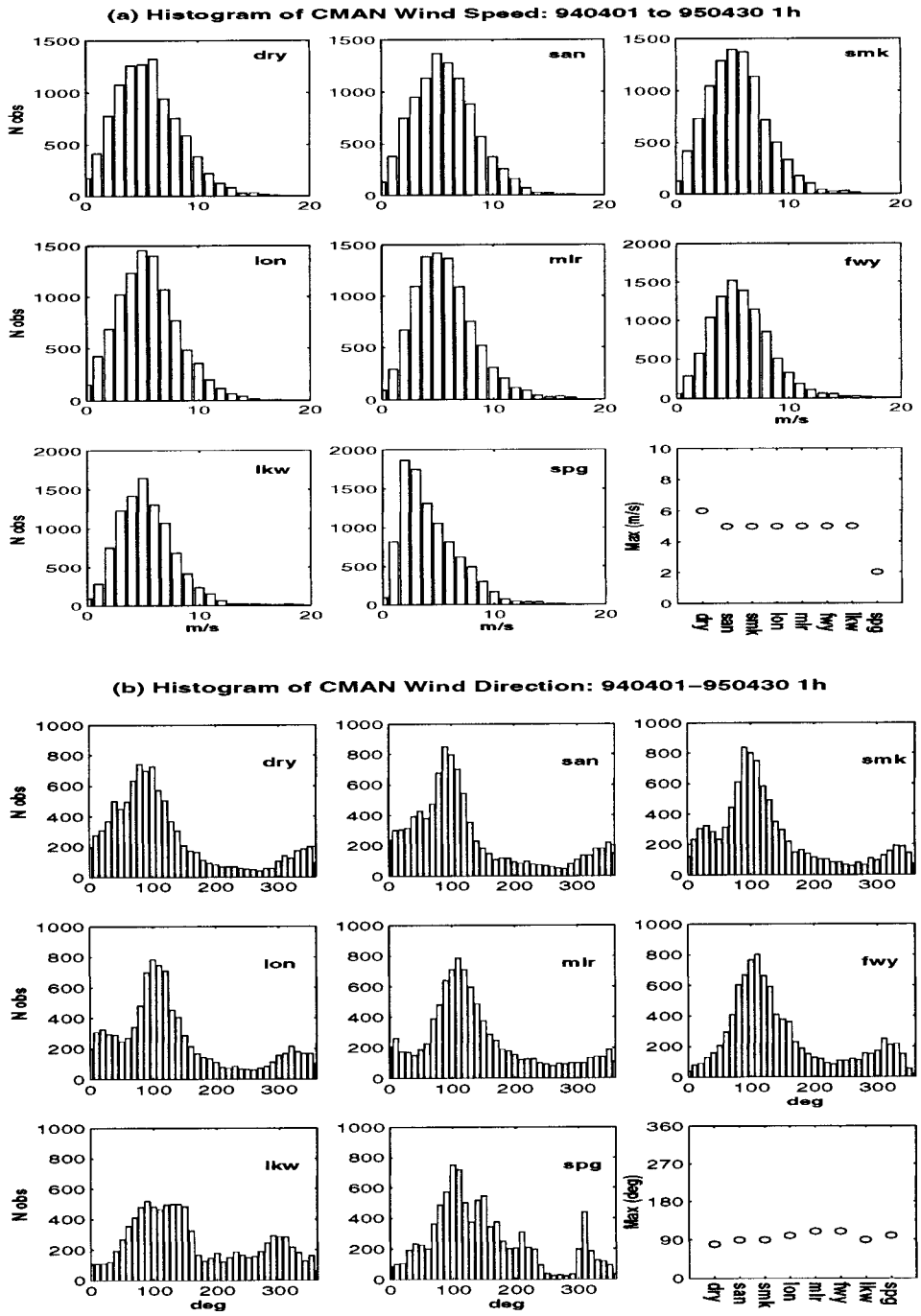

FIG. 4. The histograms of (a) wind speed (the plot at the lower-right corner shows the most frequent wind speed) and (b) wind direction (the plot at the lower-right corner shows the most frequent wind direction). The data are grouped into 1 m s^{-1} bins for wind speeds and 10° bins for directions. The stations are labeled in the plots.

In this section, 13-month records of surface winds from the 80-km grid η Model, the ASB, and a C-MAN station are analyzed statistically to examine the variability represented in the operational analysis system in comparison with the observations. Since the 12-hourly η winds do not resolve the diurnal sea–land breeze, the emphasis here is on seasonal and synoptic-scale variations displayed in the η Model versus local surface winds and on η Model bias in representing the local surface winds.

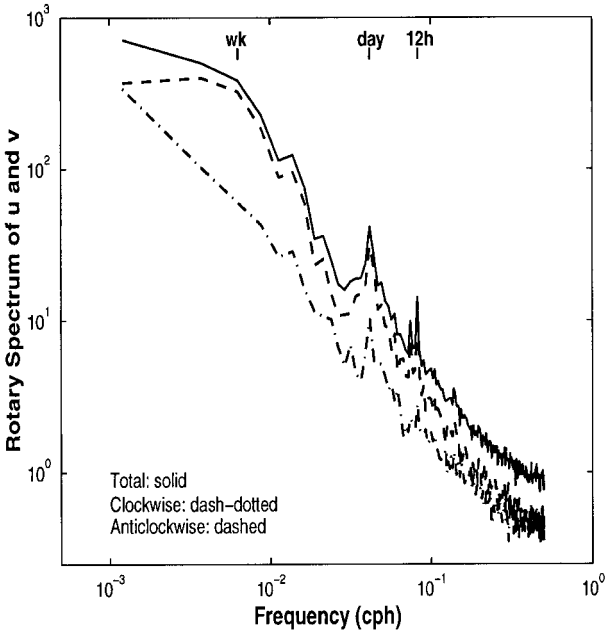

FIG. 5. Ensemble mean of rotary spectrum of horizontal velocity. The mean is calculated from the spectrum estimates for all eight C-MAN stations.

a. Data

In addition to the C-MAN winds used in the previous section, the hourly wind data for an ASB (42037) were obtained from NDBC. The 2.4-m diameter ASB was deployed at 24.51°N, 81.38°E in March 1994 by NDBC. The ASB makes oceanic, atmospheric, and wave measurements. Only surface wind measurements are analyzed here. Twelve-hourly η Model surface winds were obtained daily from NCEP through anonymous file transfer protocol (ftp) and archived locally. The η Model is a mesoscale numerical weather prediction model that uses the η coordinate for a terrain-following vertical coordinate (Mesinger et al. 1988; Black and Janjic 1988). The model became operational at NCEP in June 1993 with 80-km horizontal resolution and 38 vertical levels (Black 1994).[2] The analysis fields used to initialize the model have a 3-h window. Although the analysis scheme utilizes a vast set of observations including surface and upper-level observation networks, the local-scale flows may not be represented correctly in the model because of the model resolution and the weighting function used in the objective analysis. When a large difference between observations and model-forecasted fields occurs, the analysis scheme decides whether to reduce its weight for the observation or reject it. On average, the model wind analysis tends to be overly smooth.

The 10-m η winds are used for this study. The winds

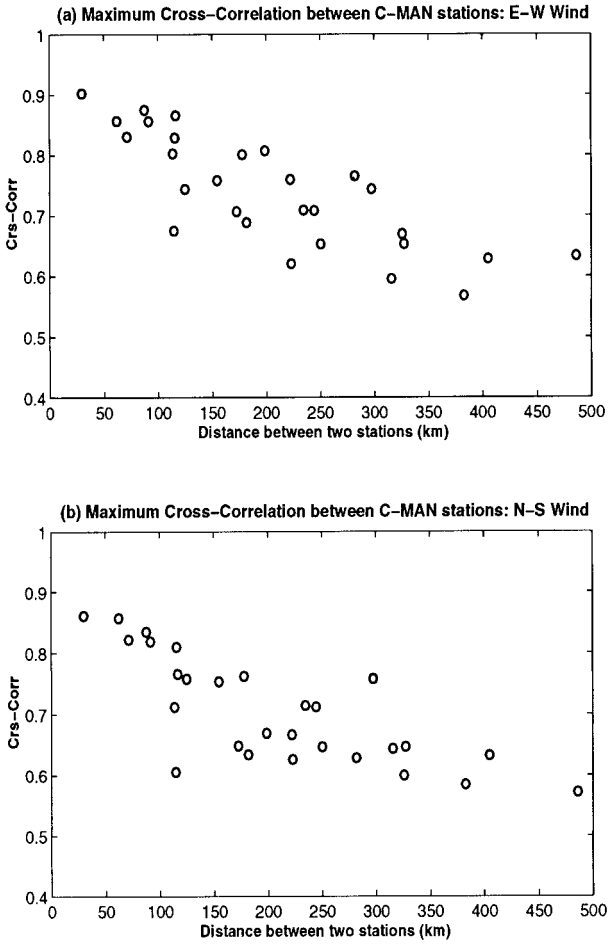

FIG. 6. The maximum cross correlation between C-MAN stations as a function of station separation for (a) u component and (b) v component.

are at 10 m above η Model ground level, which may make them different from the true 10-m winds above the ground. Since the orographic effects are minimal in south Florida, the difference should be minimal as well. The large missing data percentage for the η Model winds is caused by failures in capturing the real-time data stream from the NCEP ftp site. Linear interpolation in time is used for ASB and η winds. Both C-MAN and ASB winds are subsampled to 12-hourly values to be consistent with the η Model winds. The ASB wind speeds are adjusted to 10-m equivalent wind speed using the same procedure as was used for C-MAN winds.

b. Results

In south Florida, the winter season extends from about 15 October to 15 April and the summer season from about 15 April to 15 October; it would be ideal if both summer and winter seasonal datasets could have been so defined. However, because of local computer network and human failures, large gaps existed in the η Model winds between

[2] Since the time frame of the current study, the η Model has been rendered on higher-resolution grids.

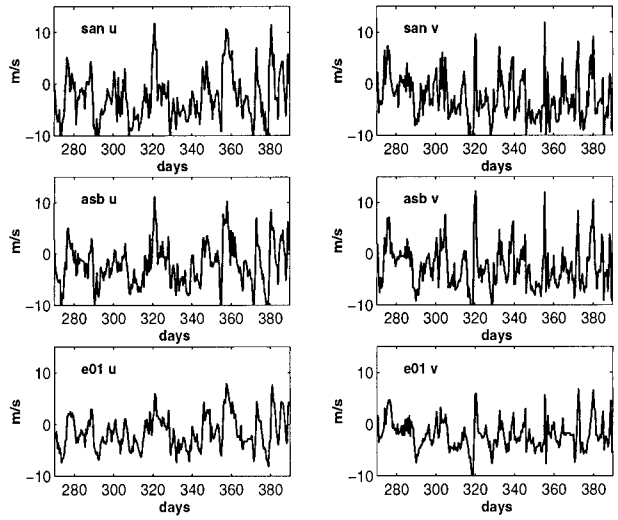

FIG. 7. Time series of u and v components for winter (27 Sep 1994–24 Jan 1995) for the Sand Key C-MAN station (two upper panels); for the air–sea interaction buoy (the two middle panels); and for the η Model grid point e01 (the two lower panels).

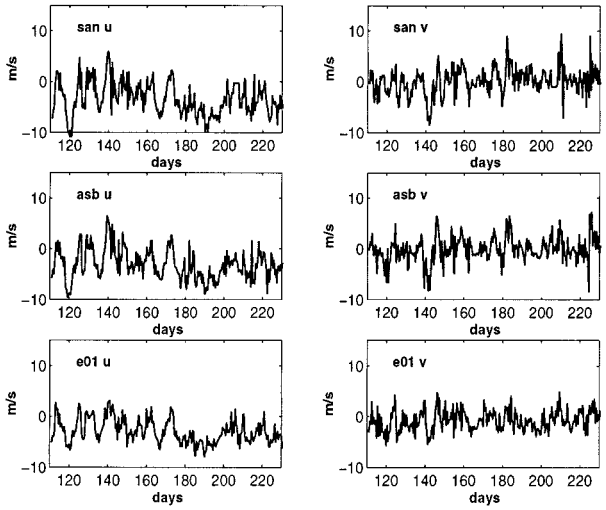

FIG. 8. Same as Fig. 7 except for summer (21 Apr 1994–18 Aug 1994).

18 August and 7 September 1994 and after 24 January 1995. Care is taken to avoid data gaps as much as possible in splitting the wind records into summer and winter seasons. For the current analysis, each season consists of about four months. The summer period is taken to be from 21 April 1994 to 18 August 1994, and the winter period to be from 7 September 1994 to 24 January 1995. These periods include the majority of the south Florida summer and winter seasons.

The results from the previous section indicated that the winds from the C-MAN network are largely statistically homogeneous along the Straits of Florida. Therefore, the wind observations at the Sand Key C-MAN station (SAN) are used to represent C-MAN winds. Hence, the focus is on the ASB, SAN, and a nearby η Model grid point (e01) which is located between the ASB and SAN and separated from the ASB by 35.5 km and from SAN by 33.5 km. (top of Fig. 1).

1) TIME SERIES AND BASIC STATISTICS

The fluctuations of the surface u and v velocity components, as expected, are larger in winter (Fig. 7) than in summer (Fig. 8; see also Tables 4 and 5). The winds from SAN, the ASB, and e01 are similar visually, but the winds from SAN and the ASB are clearly in closest agreement. The seasonal means for SAN are slightly larger than those of the ASB: about 9.25% and 5.5% for winter and summer, respectively. These differences may be caused by the different averaging methods. Since C-MAN hourly winds are based on 2-min sampled winds that are scalar averaged while the hourly ASB winds are based on 8.5-min sampled winds that are vector averaged, the mean difference with these two types of averages is around 7% (Gilhousen 1987).

The seasonal means and standard deviations for the η Model winds are smaller than for the observed winds (Tables 4 and 5). The maximum SAN (ASB) wind exceeds the maximum η Model wind by 3.8 m s^{-1} (3.2 m s^{-1}) for u and 5.0 m s^{-1} (5.5 m s^{-1}) for v in winter (Table

TABLE 4. Statistics of winds for 27 Sep 1994–24 Jan 1995 (winter). Key for datasets being compared: u and v are the zonal and meridional wind components, respectively, san is the Sand Key C-MAN station, asb is moored buoy 42037, and e01 is a nearby η Model grid point. Corr is correlation coefficient.

Station identifier	san		asb		e01	
Variables	u	v	u	v	u	v
Mean	−2.49	−2.65	−2.08	−2.56	−1.50	−2.02
STD	4.68	4.38	4.15	4.25	3.27	2.87
Max	11.73	11.79	11.12	12.15	7.90	6.70
Min	−12.83	−15.79	−11.78	−13.71	−8.10	−10.60
	u_{san}–u_{asb}	v_{san}–v_{asb}	u_{san}–u_{e01}	v_{san}–v_{e01}	u_{asb}–u_{e01}	v_{asb}–v_{e01}
Bias	−0.42	−0.10	−1.00	−0.63	−0.58	−0.54
Rms error	2.10	2.00	2.71	2.61	2.09	2.37
Corr	0.90	0.89	0.86	0.84	0.88	0.86

TABLE 5. Same as Table 4 but for 21 Apr 1994–18 Aug 1994 (summer).

Station identifier	san		asb		e01	
Variables	u	v	u	v	u	v
Mean	−3.25	0.13	−3.07	−0.09	−2.89	−0.78
STD	3.44	2.71	3.04	2.62	2.38	2.08
Max	5.95	9.46	6.44	7.23	3.10	4.80
Min	−10.89	−8.44	−9.51	−8.37	−7.90	−5.70
	u_{san}–u_{asb}	v_{san}–v_{asb}	u_{san}–u_{e01}	v_{san}–v_{e01}	u_{asb}–u_{e01}	v_{asb}–v_{e01}
Bias	−0.15	0.23	−0.33	0.91	−0.18	0.69
Rms error	1.84	1.90	2.20	2.47	1.71	2.26
Corr	0.85	0.75	0.78	0.57	0.83	0.60

4) and 2.9 m s^{-1} (3.3 m s^{-1}) for u and 4.7 m s^{-1} (2.4 m s^{-1}) for v in summer (Table 5). A bias of up to 2 m s^{-1} exists in the monthly means (Fig. 9) and of up to 1 m s^{-1} in the seasonal means (Tables 4 and 5). Thus, the η Model gridcell wind speed significantly underestimates the pointwise surface wind speed in this region.

2) CROSS CORRELATION, SPECTRA, COHERENCE, AND PHASE

The maximum cross correlations (which occur at zero time lag) of SAN versus the ASB are higher than either versus e01. They also are higher in winter than in summer, substantially so for the meridional component (Tables 4 and 5). The maximum cross correlations for the ASB versus the η winds are somewhat higher than those for SAN versus the η winds.

The SAN and ASB total wind spectra are in closest agreement. The η Model total wind spectra are less energetic, even at periods longer than three days (Fig. 10).

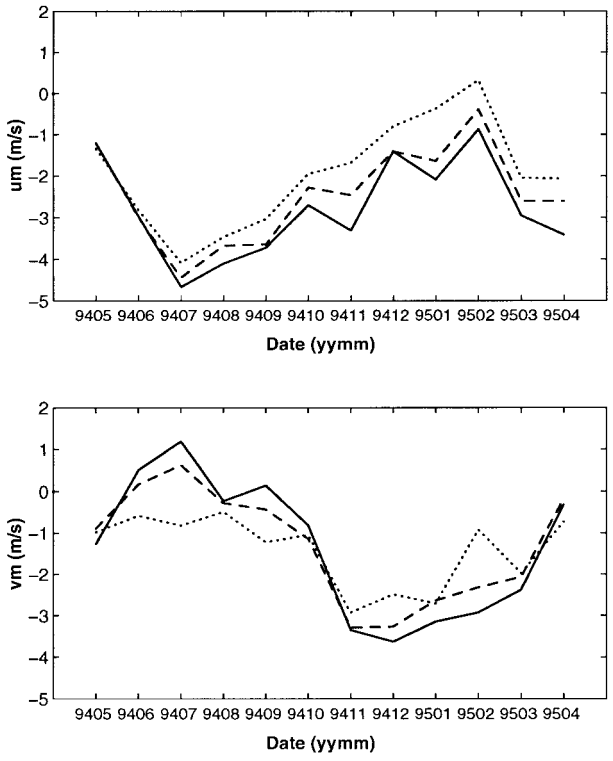

FIG. 9. Monthly means of u (upper panel) and v components (lower panel). Solid lines are for the Sand Key C-MAN station; dashed lines are for the air–sea interaction buoy; and dotted lines are for the η Model grid point e01.

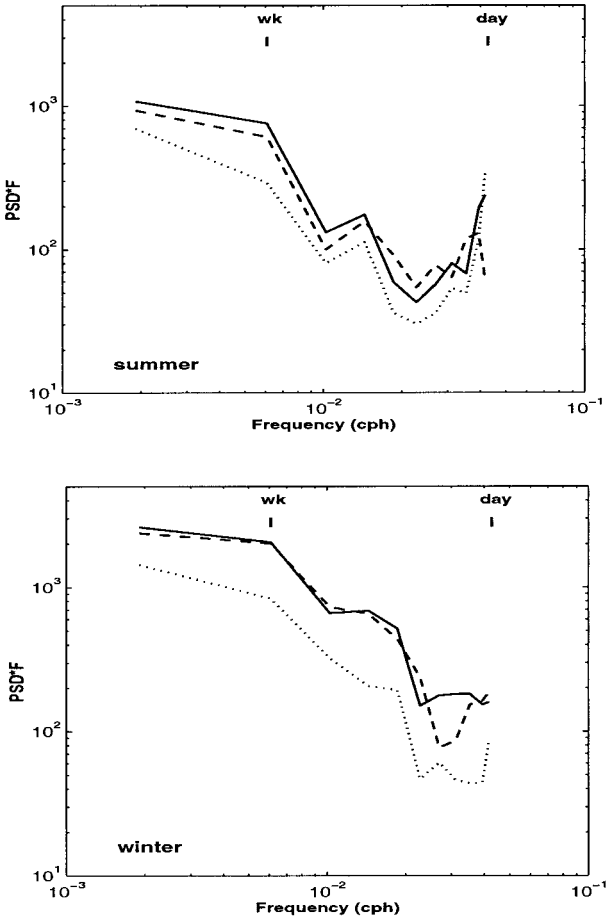

FIG. 10. Total wind spectra for winter (lower panel) and summer (upper panel).

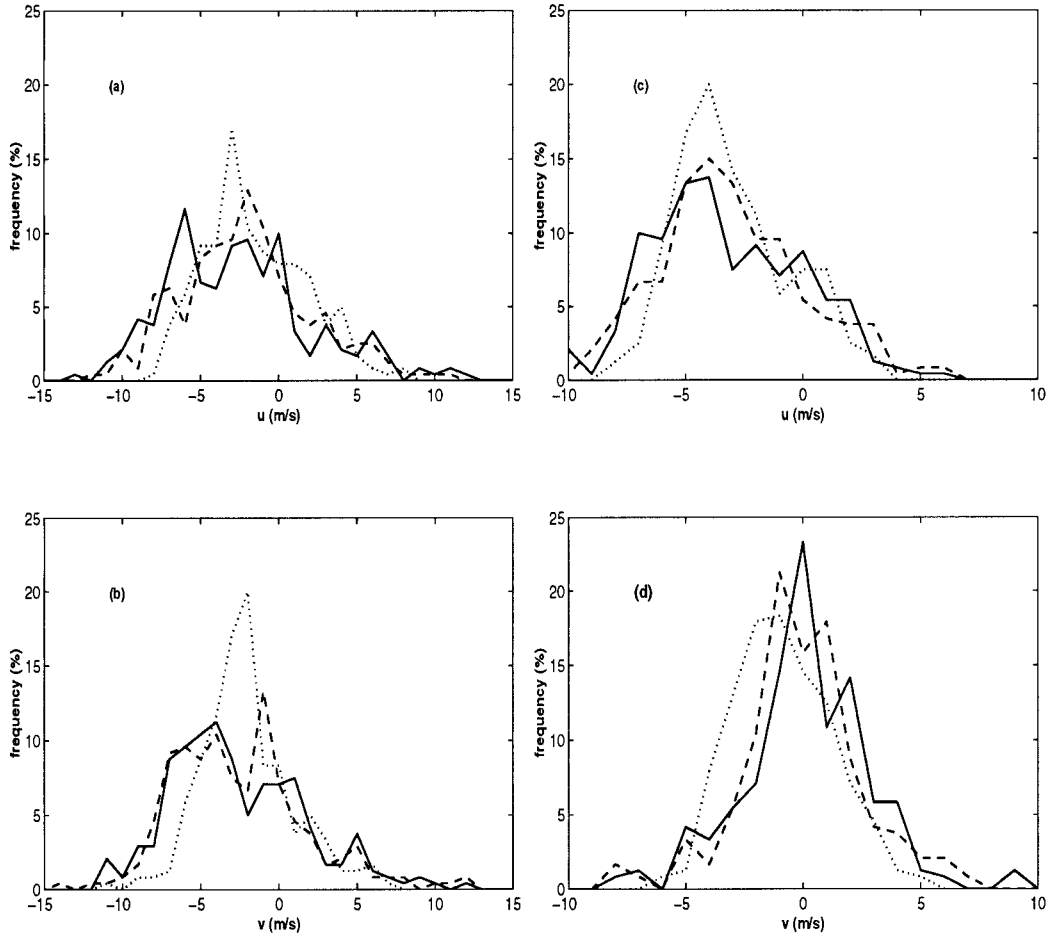

FIG. 11. Histograms of the u and v wind components for the Sand Key C-MAN station (solid lines), air–sea interaction buoy (dashed lines), and the η Model grid point e01 (dotted lines) for (a) and (b) winter and for (c) and (d) summer.

The η Model total wind spectra agree more closely with the observed total wind spectra in summer than in winter.

For timescales between 3 days and 3 weeks, the SAN, ASB, and η winds have a coherence greater than 0.8 and are nearly in phase (difference is less than 15°; figure not shown).

3) HISTOGRAMS

The histograms for the η wind components are smoother and more symmetric (Fig. 11) and decrease more rapidly with speed than those of the SAN and ASB wind components.

TABLE 6. Chi-square test results. Variables are defined in section 3b3. Key for datasets being compared: u and v are the east–west and north–south wind components, respectively, san is the Sand Key C-MAN station, asb is moored buoy 42037, and e01 is a nearby η Model grid point.

Datasets		Summer			Winter		
		ν	x^2	$Q(x^2/\nu)$	ν	x^2	$Q(x^2/\nu)$
u_{san}	u_{asb}	18	22.05	0.23	26	31.44	0.21
u_{san}	u_{e01}	18	39.24	$\leq$0.01	25	71.53	$\ll$0.01
u_{asb}	u_{e01}	17	31.05	0.02	24	43.52	$\leq$0.01
v_{san}	v_{asb}	16	26.17	0.05	27	19.19	0.86
v_{san}	v_{e01}	16	58.38	$\ll$0.01	24	68.95	$\ll$0.01
v_{asb}	v_{e01}	16	46.89	$\ll$0.01	25	66.74	$\ll$0.01

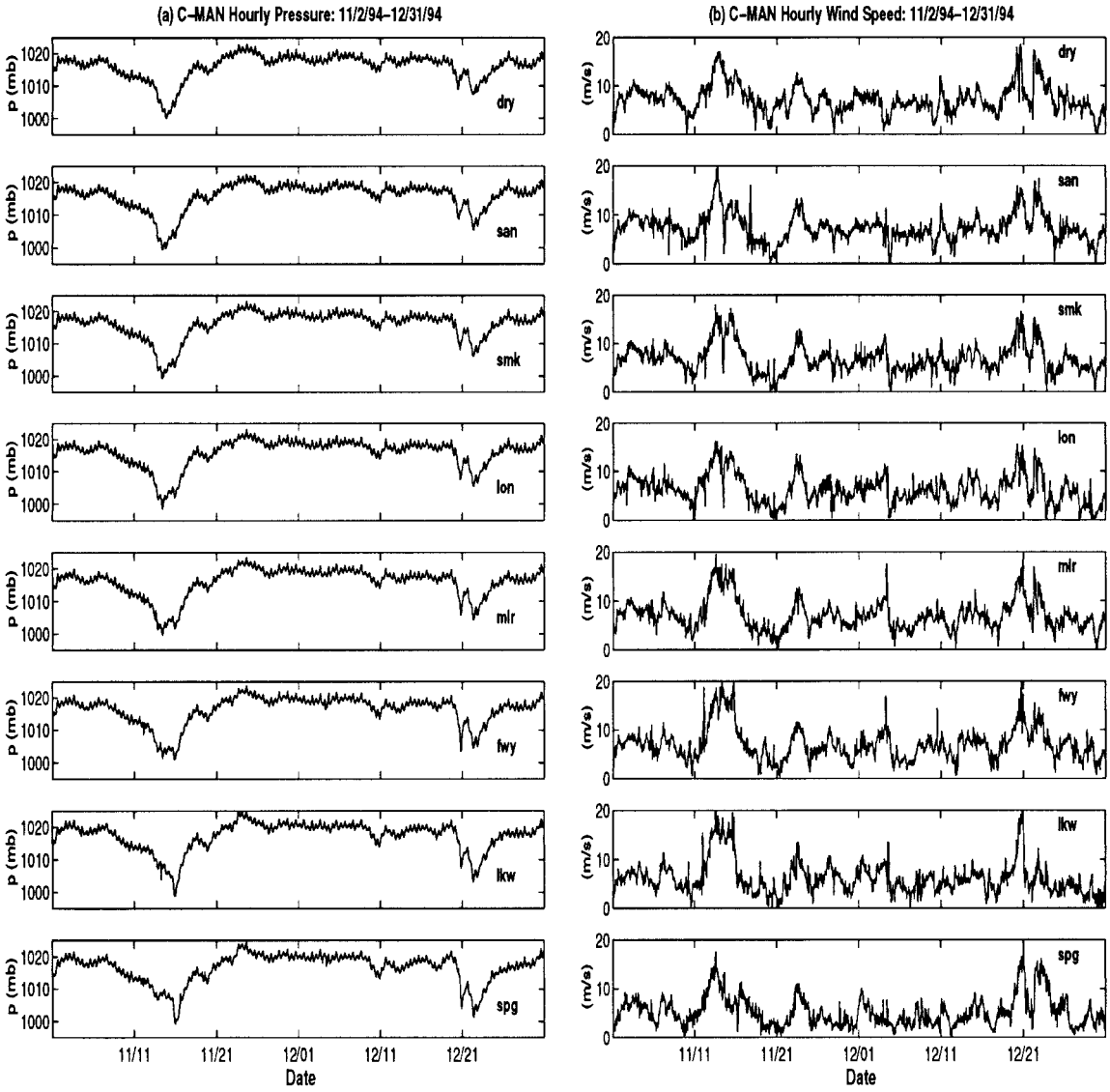

FIG. 12. Time series of C-MAN hourly (a) surface pressure and (b) surface wind speeds for Nov and Dec 1994.

In winter (Figs. 11a,b), largely influenced by frontal passages, both SAN and ASB winds are distributed over a broader range than in summer (± 15 m s^{-1} vs ± 10 m s^{-1}). SAN u has three major peaks (near -6, -2, and nearly zero m s^{-1}) and v has two major peaks (near -4 and 1 m s^{-1}, respectively). The ASB u has a major peak at 2 m s^{-1} and v has three distinct peaks (near -7, -4, and -1 m s^{-1}). For the η winds, both u and v histograms deviate from the observed histograms by a wide margin; for example, they have only one peak at -3.5 and -2.5 m s^{-1}, respectively.

In summer (Figs. 11c,d), mainly influenced by local sea–land breezes with occasional tropical disturbances superimposed, the histograms for these three sets of winds are most consistent visually for u. The η Model histogram is biased for v; its peak is shifted to -2 m s^{-1} from zero compared with SAN and -1 m s^{-1} compared with the ASB.

Do the frequency distributions for these three datasets follow the same distribution function? The chi-square test is performed to answer this question. The methodology and programs are based on Press et al. (1992). Let R_i be the number of occurrences in the ith bin for the first dataset, and S_i be the number of occurrences in the same bin for the second dataset; the chi-square statistic then is defined as

$$\chi^2 = \sum_i \frac{(R_i - S_i)^2}{R_i + S_i}.$$

If ν is the number of degrees of freedom, $Q(\chi^2 \mid \nu)$ is the chi-square probability function, which is an incomplete gamma function defined as

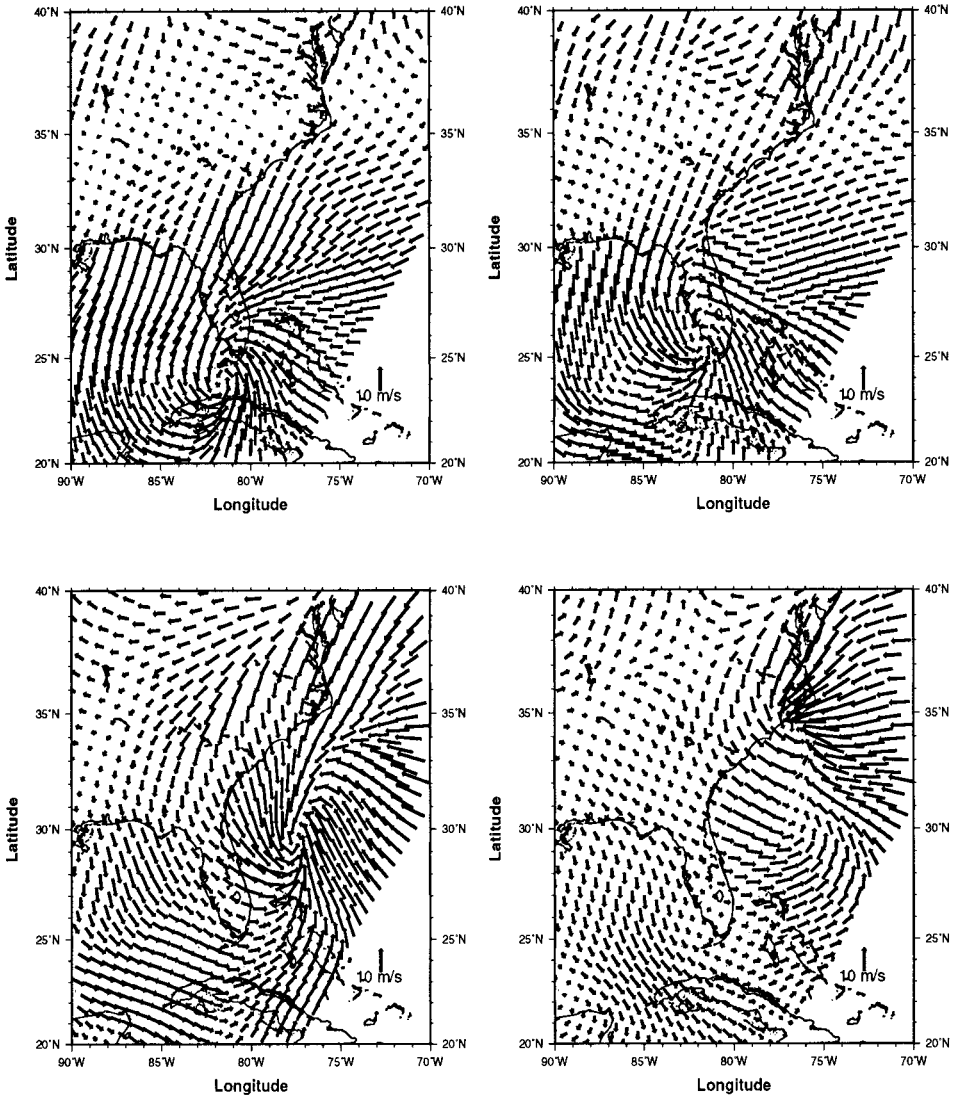

FIG. 13. Surface wind vectors from the η Model for Tropical Storm Gordon from 1200 UTC 15 Nov to 1200 UTC 18 Nov 1994 every 24 h, left to right, then top to bottom.

$$Q(\chi^2 \mid \nu) \equiv \frac{1}{\Gamma(\chi^2)} \int_{\nu}^{\infty} e^{-t} t^{\chi^2 - 1}\, dt$$

where Γ is the gamma function defined by the integral

$$\Gamma(x) = \int_0^{\infty} t^{x-1} e^{-t}\, dt$$

and t is the integration variable.

At the significance level of 0.05, results shown in Table 6 (above) indicate that the closeness of distributions for SAN and the ASB is acceptable for both u and v in both summer and winter, but more so for the v component in winter. It is obvious that the distribution functions for the η Model winds are statistically different from either the distribution function of SAN winds or that of the ASB winds. The best value of the chi-square probability function is 0.02 for the distributions of u component between the ASB and e01 in summer.

4. Spatial variability in wind fields of synoptic-scale weather events

The annual march of south Florida weather is influenced by multiscale processes. The North Atlantic subtropical high sets the large-scale regime and drives the trade winds. Tropical easterly waves and cyclones in summer and extratropical cyclones associated with cold front passages in winter superimpose synoptic-scale winds onto the large-scale winds. Tropical Storm Gordon, which occurred in November 1994, and a frontal passage that occurred in December 1994, are two such

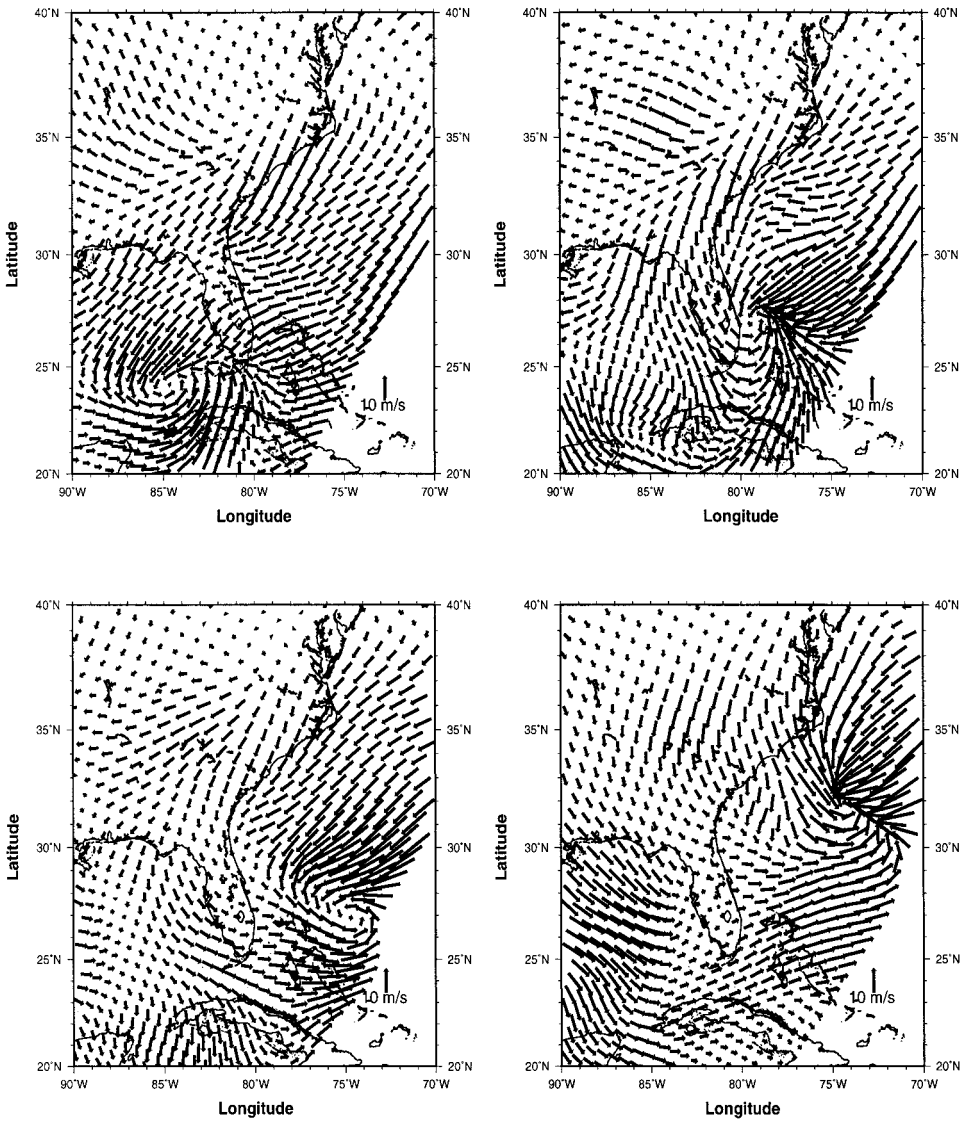

FIG. 14. Surface wind vectors from the η Model for the extratropical cyclone from 1200 UTC 21 Dec to 0000 UTC 23 Dec 1994 every 12 h, left to right, then top to bottom.

synoptic-scale events captured in the record for the south Florida domain.

a. Description of synoptic events

1) TROPICAL STORM GORDON

In November 1994, Tropical Storm Gordon originated in the western Caribbean Sea south of Yucatan, Mexico. The pressure dropped over 25 hPa along the track and the observed maximum wind speed reached over 30 m s^{-1}. It crossed Florida Bay and central Florida, and then curved back to the northeast coast of Florida after it had headed into the North Atlantic. As Gordon moved through Florida Bay, all eight C-MAN stations experienced a sharp pressure drop (about 20 hPa) and a wind burst (up to 20 m s^{-1}; Fig. 12). A well-organized circulation was represented in the η winds (Fig. 13).

2) EXTRATROPICAL CYCLONE

In December 1994, an extratropical cyclone developed at the tail of a diffuse extratropical front in the Gulf of Mexico and passed through the south Florida domain rapidly. Again, a distinct pressure drop and a wind change, equivalent to the ones associated with Gordon, were experienced at all eight C-MAN stations (Fig. 12). The southern stations experienced a smaller pressure drop than the northern stations (10 hPa compared with 20 hPa) because of the relative location of each individual station. The η Model captured the sharp wind shear associated with the front (Fig. 14).

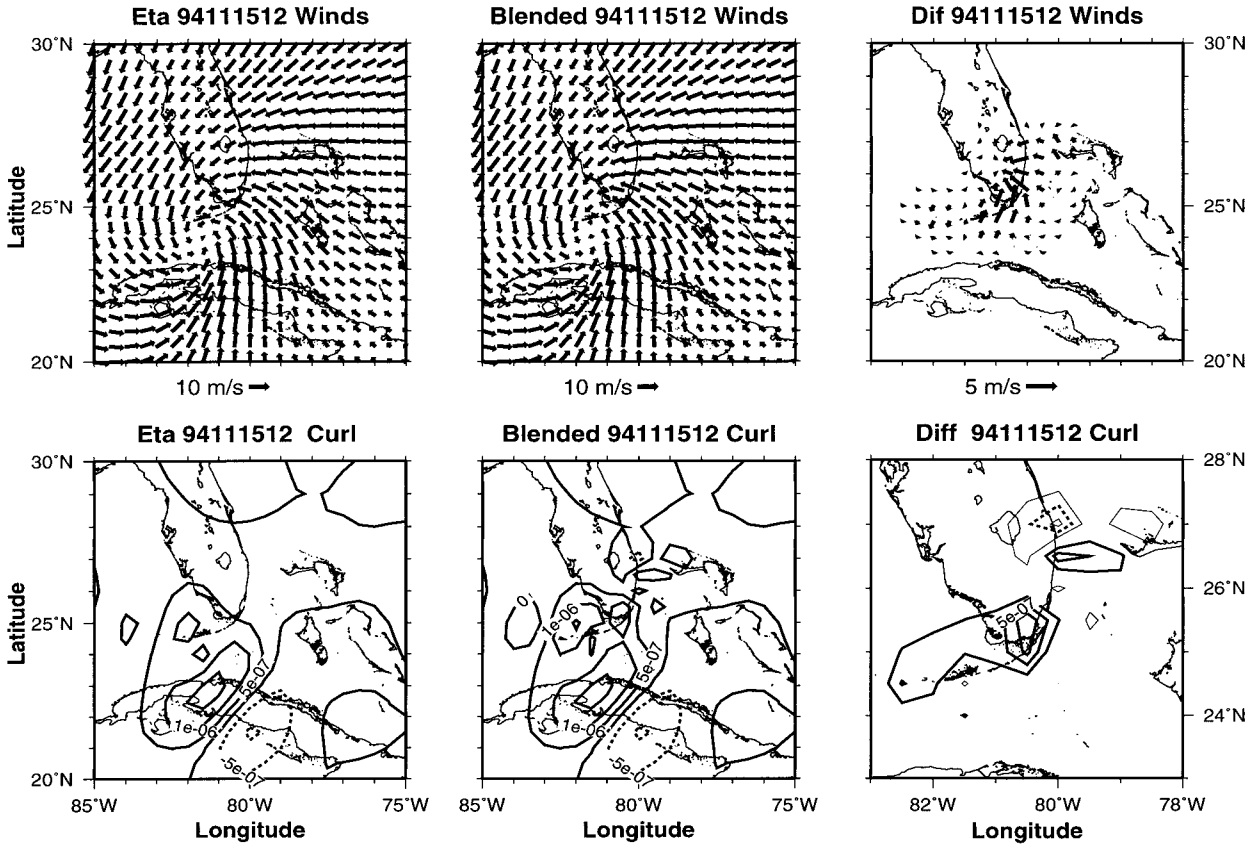

FIG. 15. Surface wind vectors and wind-stress curl fields for η winds, blended winds, and the difference between the two for 1200 UTC 15 Nov 1994. The vector scales are shown under the plots. The contour interval is 5×10^{-7} N m^{-3} for the curl of η and blended wind-stress fields and 2.5×10^{-7} N m^{-3} for the difference. The plotting domain for the difference curl is reduced to display better the structure in the subdomain of most interest.

b. Blended winds

The surface winds from the C-MAN and ASB stations are influenced by smaller-scale variability than are the η winds, but this local observational network does not provide information on a regional scale as the η Model does. Spatial variability supplied by the network may be lost during the model analysis procedure. By combining the model and observed winds, there is the possibility of providing a wind field on a regional scale with more local small-scale spatial variability. How much of such information will emerge in the blended field? Is it significant in magnitude? Those questions are addressed in this section. The local circulation within about 100 km of the C-MAN and ASB sites will be most affected by the additional information they provide. Using η winds as the background field, winds from the C-MAN and ASB stations are blended into the η winds with a spline-fitting scheme (Chin et al. 1998).

Since the vertical component of the wind-stress curl is a primary driving force on the ocean surface, it also is computed. Using a bulk formula, the wind stress on the ocean surface is computed here as

$$\boldsymbol{\tau} = \rho_a C_D |\mathbf{V}| \mathbf{V},$$

where $\mathbf{V} = u\mathbf{i} + v\mathbf{j}$ are horizontal velocity, $|\mathbf{V}| = \sqrt{u^2 + v^2}$ is the wind speed, and ρ_a is the standard sea level air density; C_D is the neutral 10-m drag coefficient given by Large and Pond (1981) that is defined as

$$C_D = \begin{cases} 0.00118 & \text{if } |\mathbf{V}| \le 10 \text{ m s}^{-1} \\ 0.00049 + 0.000069|\mathbf{V}| & \text{otherwise.} \end{cases}$$

If the spatial variations of C_D are ignored, the wind-stress curl on the ocean surface then is defined as (Chin et al. 1998)

$$\nabla_z \times \boldsymbol{\tau} = \rho_a C_D \left\{ |\mathbf{V}| \left(\frac{\partial v}{\partial x} - \frac{\partial u}{\partial y} \right) + |\mathbf{V}|^{-1} \left[v^2 \frac{\partial v}{\partial x} - u^2 \frac{\partial u}{\partial y} + uv \left(\frac{\partial u}{\partial x} + \frac{\partial v}{\partial y} \right) \right] \right\}. \quad (3)$$

The η winds capture the overall flow patterns in both tropical and extratropical storm events (Figs. 15 and 16), respectively. However, the differences between η-only and blended wind fields indicate that local observed winds and shear are stronger in both cases. Residual

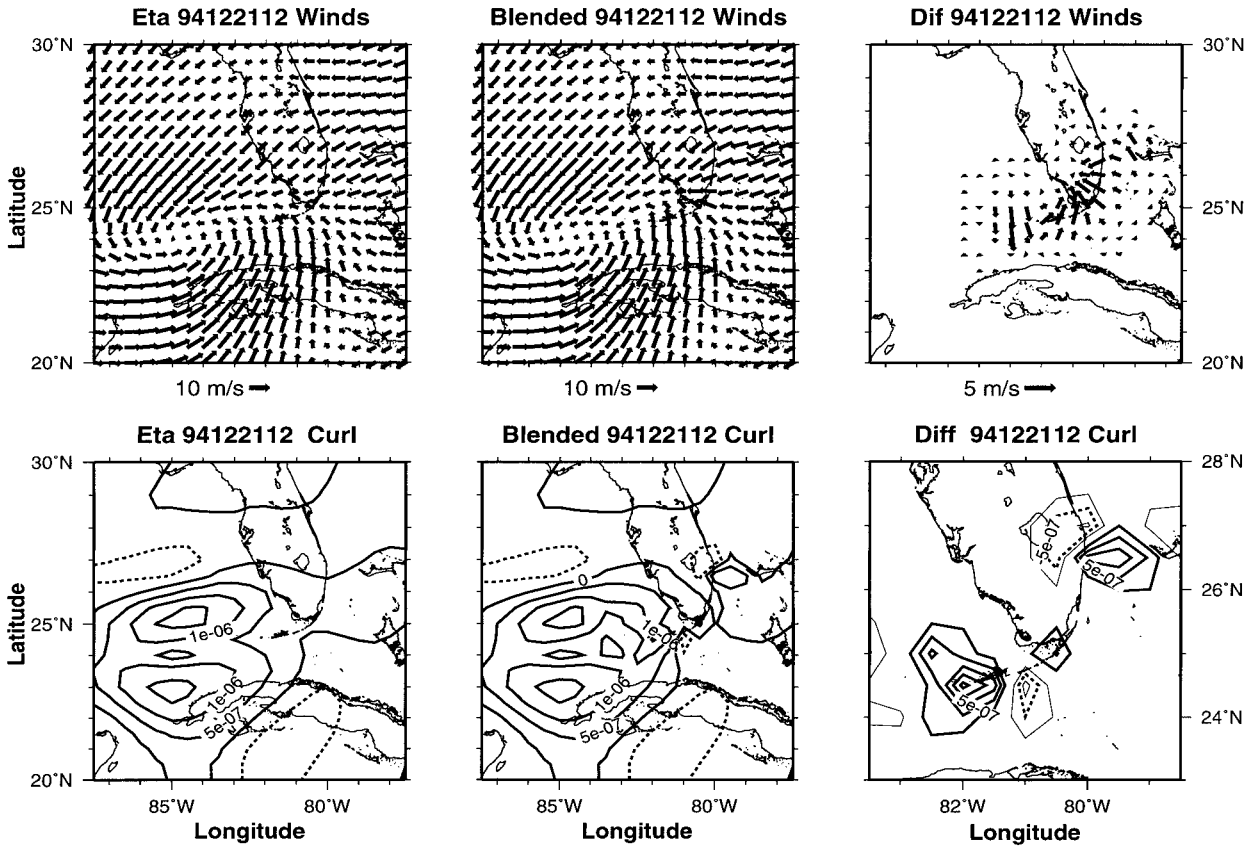

FIG. 16. Same as Fig. 15 but for 1200 UTC 21 Dec 1994.

wind-stress curl fields display a relatively weak but distinct pattern associated with this shear, which is not resolved by the η winds and which is on the order of the total curl in magnitude. The maximum centers of the residual wind-stress curl are located near the coast and may affect wind-driven coastal circulation, which in turn could affect estimates of Lagrangian transports along the Straits of Florida and in and out of the Florida Bay. The impact such wind-stress (and its curl) residuals would have on regional ocean circulation needs to be examined in the future using an eddy-resolving ocean circulation model.

5. Summary

Based on a statistical analysis of coastal winds and other variables from eight south Florida C-MAN stations, the surface observational network was found to be fairly homogeneous along the Straits of Florida. The wind speed and direction histograms and monthly means among Sand Key, Sombrero, Long Key, and Molasses stations are similar. The C-MAN winds reveal seasonal cycles in monthly mean winds and standard deviations that vary systematically along the Straits of Florida. The correlation values between adjacent station pairs are high, ranging from 0.9 to 0.75 over separations of 30–117 km, respectively; thus, the C-MAN stations are highly coherent. The ensemble mean rotary spectra of winds show distinct peaks at semidiurnal and diurnal frequencies, and a broad peak at the weather band (4–7 days) in the anticlockwise spectrum.

Because of a lengthy gap, the records at Venice were not used. Thus, the cross-coast variability was not addressed. As extratropical and tropical weather systems advance across the south Florida region from both coasts, the cross-coast variability may play a large role in local weather forecasting. In light of that possibility, redistribution of the existing alongcoast C-MAN stations should be considered so as to provide better spatial coverage without losing too much of the synoptic and large-scale information that they currently provide. Of course, such action should proceed with caution because for certain studies (e.g., ecosystem or hurricane landfall) the present C-MAN station distribution may be more desirable.

The 80-km η winds compare well with the observed C-MAN and ASB winds except in the following aspects. The η Model tends to underestimate wind speeds, which results in less energetic spectra. A bias was found in the η meridional component: stronger southward winds than the nearby observed winds were simulated. Also, the η wind histograms are smoother than is observed.

The η Model produces circulation patterns typical of weather systems in south Florida quite well but underestimates wind speed, which may cause the surface wind-stress curl over the coastal ocean to be misrepresented. Observations from local wind measurements such as C-MAN and buoys could enhance the quality of model winds; together they can provide more accurate wind estimates. Thus, the local observation network still is essential in augmenting the regional model-based wind fields. In examining the η Model winds, little evidence is seen that the local surface observations are assimilated. For the η Model to produce an accurate wind field on the local scale, these available buoy data should receive more attention. The same suggestion has been made in an ocean wave modeling study (Cardone et al. 1995). Since models evolve rapidly, these issues need to be reexamined periodically with upgraded versions of NCEP's operational models.

Acknowledgments. This work was supported by the U.S. Coast Guard and NOAA's Coastal Ocean Program through the South Florida Oil Spill Research Center, a program of the University of Miami's Ocean Pollution Center. The ASB and C-MAN data were downloaded and decoded by Ram Vakkayil. Ian Palno from NDBC provided the March 1995 data for Sombrero Key. The η Model surface winds were decoded and archived by Dong-Shan Ko. We thank Mark Bushnell (AOML/NOAA), Sandra L. Vargo (FIO), and David Forcucci (FIO, currently RSMAS/UM) for information on the C-MAN stations, Jiann-Gwo Jiing (NHC, Miami) for the information on the south Florida NWS stations, and William Syrett (PSU) for providing the daily weather maps for the extratropical cyclone event. Discussions with Kevin Leaman (RSMAS/UM) on statistical analysis and Arthur Mariano (RSMAS/UM) on data analysis were beneficial. Figures 13–16 were generated using the GMT graphics package. Renellys Perez coded the chi-square test. Comments from Mark Powell (AOML/NOAA) and two anonymous reviewers have improved the clarity of the paper.

REFERENCES

Black, T. L., 1994: The new NMC mesoscale η Model: Description and forecast examples. *Wea. Forecasting,* **9,** 265–278.

——, and Z. I. Janjic, 1988: Preliminary forecast results from a step-mountain η coordinate regional model. Preprints, *Eighth Conf. on Numerical Weather Prediction,* Baltimore, MD, Amer. Meteor. Soc., 442–447.

Blanchard, D. O., and R. E. López, 1985: Spatial patterns of convection in south Florida. *Mon. Wea. Rev.,* **113,** 1282–1299.

Bosart, L. F., and W. A. Sprigg, 1998: *The Meteorological Buoy and Coastal Marine Automated Network for the United States.* National Academy Press, 97 pp.

Burpee, R. W., 1979: Peninsula-scale convergence in the south Florida sea breeze. *Mon. Wea. Rev.,* **107,** 852–860.

Byers, H. R., and H. R. Rodebush, 1948: Causes of thunderstorms of the Florida peninsula. *J. Meteor.,* **5,** 275–280.

Cardone, V. J., 1969: Specification of the wind distribution in the marine boundary layer for wave forecasting. Rep. TR69-1, New York University, 131 pp.

——, J. A. Greenwood, and M. A. Cane, 1990: On trends in historical marine wind data. *J. Climate,* **3,** 113–127.

——, H. Graber, R. E. Jensen, S. Hasselmann, and M. J. Caruso, 1995: In search of the true surface wind field in SWADE IOP-1: Ocean wave modelling perspective. *Global Atmos. Ocean Syst.,* **3,** 107–150.

Chin, T. M., R. F. Miliff, and W. G. Large, 1998: Basin-scale, high-wavenumber sea surface wind fields from a multiresolution analysis of scatterometer data. *J. Atmos. Oceanic Technol.,* **15,** 741–763.

Cooper, H. J., M. Garstang, and J. Simpson, 1982: The diurnal interaction between convection and peninsular-scale forcing over south Florida. *Mon. Wea. Rev.,* **110,** 486–503.

Cressman, G., 1959: An operational objective analysis system. *Mon. Wea. Rev.,* **87,** 367–374.

Cunning, J. B., R. L. Holle, P. T. Gannon Sr., and A. T. Watson, 1982: Convective evolution and merger in the FACE experimental area: Mesoscale convection and boundary layer interactions. *J. Appl. Meteor.,* **21,** 953–977.

Fratantoni, P. S., 1998: The formation and evolution of Tortugas eddies in the southern Straits of Florida and Gulf of Mexico. Ph.D. dissertation, University of Miami, 182 pp.

Gilhousen, D. B., 1987: A field evaluation of NDBC moored buoy winds. *J. Atmos. Oceanic Technol.,* **4,** 94–104.

——, 1988: Quality control of meteorological data from automated marine stations. Preprints, *Fourth Int. Conf. on Interactive Information and Processing System for Meteorology, Oceanography, and Hydrology,* Miami, FL, Amer. Meteor. Soc., 113–117.

Large, W. G., and S. Pong, 1981: Open ocean momentum flux measurements in moderate to strong winds. *J. Phys. Oceanogr.,* **11,** 324–336.

Lyons, W. A., R. L. Walko, M. E. Nicholls, R. A. Pielke, W. R. Cotton, C. S. Keen, and A. Watson, 1992: Observational and numerical modeling investigations of Florida thunderstorms generated by multiscale surface thermal forcing. Preprints, *Fifth Conf. on Mesoscale Processes,* Atlanta, GA, Amer. Meteor. Soc., 85–90.

Maul, G. A., S. R. Baig, and M. Bushnell, 1991: Nowcasting cross-stream profiles of ocean surface current in the Straits of Florida. *J. Atmos. Oceanic Technol.,* **8,** 179–185.

Mesinger, F., Z. I. Janjic, S. Nickovic, D. Gavrilov, and D. G. Deaven, 1988: The step-mountain coordinate model description and performance for cases of Alpine lee cyclogenesis and for a case of Appalachian redevelopment. *Mon. Wea. Rev.,* **116,** 1493–1518.

Michaels, P. J., R. A. Pielke, J. T. McQueen, and D. E. Sappington, 1987: Composite climatology of Florida summer thunderstorms. *Mon. Wea. Rev.,* **115,** 2781–2791.

Mooers, C. N. K., 1973: A technique for the cross spectrum analysis of pairs of complex-valued time series, with emphasis on properties of polarized components and rotational invariants. *Deep-Sea Res.,* **20,** 1129–1141.

——, and D. Ko, 1994: Nowcast system development for the Straits of Florida. *Estuarine and Coastal Modeling III,* M. L. Spaulding, K. Bedford, A. Blumberg, R. Chong, and C. Swanson, Eds., ASCE, 158–171.

NDBC, 1993: Coastal-Marine Automated Network (C-MAN) users guide. NOAA 1203-01.04-2B, Stennis Space Center, 55 pp.

Ogden, J. C., J. W. Porter, N. P. Smith, A. M. Szmant, W. C. Jaap, and D. Forcucci, 1994: SEAKEYS: A long-term interdisciplinary study of the Florida Keys seascape. *Bull. Mar. Sci.,* **54,** 1059–1071.

Ortner, P. B., and Coauthors, 1995: Mississippi River flood waters that reached the Gulf Stream. *J. Geophys. Res.,* **100** (7), 13 595–13 601.

Peng, G., C. N. K. Mooers, and H. C. Graber, 1996: Statistical characteristics of south Florida Coastal-Marine Automatic Network data. OPEL/RSMAS Tech. Rep., Ocean Prediction Experimental Laboratory, University of Miami, 33149, 24 pp.

Pielke, R. A., A. Song, P. J. Michaels, W. A. Lyons, and R. W. Arritt, 1990: The predictability of sea breeze–generated thunderstorms. *Atmósfera*, **4,** 65–78.

Press, W. H., S. A. Teukolsky, W. T. Vetterling, and B. P. Plannery, 1992: *Numerical Recipes in FORTRAN—The Art of Scientific Computing.* 2d. ed. Cambridge University Press, 963 pp.

Ross, D. B., V. J. Cardone, J. Overland, R. McPherson, W. J. Pierson, and S. Yu, 1985: Oceanic surface winds. *Advances in Geophysics*, Vol. 27, Academic Press, 101–139.

Segal, M., R. Avissar, M. C. McCumber, and R. A. Pielke, 1988: Evaluation of vegetation effects on the generation and modification of mesoscale circulations. *J. Atmos. Sci.,* **45,** 2268–2292.

Taylor, J. R., 1982: *An Introduction to Error Analysis—The Study of Uncertainties in Physical Measurements.* University Science Books, 270 pp.

Wang, J. D., J. van de Kreeke, N. Krishnan, and D. Smith, 1994: Wind and tide response in Florida Bay. *Bull. Mar. Sci.,* **54,** 579–601.